Heliyon 5 (2019) e02755

Contents lists available at ScienceDirect

Heliyon

journal homepage: www.heliyon.com

Heliyon

Research article

Developing an elegant and integrated electrochemical-theoretical approach for detection of DNA damage induced by 4-nonylphenol

Kazhal Ghanbari [a], Mahmoud Roshani [a,**], Hector C. Goicoechea [b], Ali R. Jalalvand [c,*]

[a] Department of Chemistry, Ilam University, Ilam, Iran
[b] Laboratorio de Desarrollo Analítico y Quimiometría (LADAQ), C_atedra de Química Analítica I, Universidad Nacional del Litoral, Ciudad Universitaria, CC 242 (S3000ZAA), Santa Fe, Argentina
[c] Research Center of Oils and Fats, Kermanshah University of Medical Sciences, Kermanshah, Iran

ARTICLE INFO

Keywords:
Analytical chemistry
Electrochemistry
DNA damage
Electrochemical biosensor
4-nonylphenol

ABSTRACT

In this work, a novel biosensor was fabricated for detection of DNA damage induced by 4-nonylphenol (NP) and also determination of NP. To achieve this goal, a glassy carbon electrode (GCE) was modified with chitosan (Chit), gold nanoparticles (Au NPs) and DNA-multiwalled carbon nanotubes (DNA-MWCNTs). Then, the DNA-MWCNTs/Au NPs/Chit/GCE was incubated with methylene blue (MB) to obtain MB-DNA-MWCNTs/Au NPs/Chit/GCE in which MB was used as the redox indicator. The modifications applied to the GCE were characterized by cyclic voltammetry (CV), electrochemical impedance spectroscopy (EIS), scanning electron microscopy (SEM), energy dispersive X-ray spectroscopic (EDS) and theoretical evidence. MB is a derivative of anthraquinone which can intercalate into double helix structure of DNA. By treating MB-DNA-MWCNTs/Au NPs/Chit/GCE with NP, a higher R_{ct} was observed because the insertion of the NP may result in a more negative charge environment on the DNA surface which hinders accessibility of $[Fe(CN)_6]^{3-/4-}$ anion to the electrode surface. Change in the EIS response of the biosensor in the presence of NP was used to develop a novel system for monitoring the DNA damage induced by NP. The EIS technique was also used to develop a sensitive electroanalytical method for determination of NP.

1. Introduction

Deoxyribonucleic acid (DNA) is one of the four important types of biomacromolecules which are essential in life processes. Only a part of DNA (less than 2%for humans) is coding, meaning that these sections stores and encodes genetic information [1]. Therefore, DNA has a critical role in cellular processes and functioning of all types of organisms and many viruses for survival [2]. Numerous chemical and/or physical factors, including high temperature, ionizing radiations, heavy metal ions and many of chemicals in our environment can induce damage to the DNA sequence and cause changes in the chemical structure of the DNA molecule [3, 4, 5, 6, 7]. DNA damage is an abnormal chemical structure in DNA leading to mutagenesis and carcinogenesis which can induce several diseases such as cancer, tumor, diabetes, hypertension and arteriosclerosis [8, 9, 10, 11]. Endocrine disrupting chemicals are one of the chemicals that can induce DNA damage and interfere with the endocrine system. 4-nonylphenol (NP) as a member of the endocrine disrupters is extensively used as nonionic surfactants in a variety of industrial and agricultural products. This disruptor causes various problems in the normal, hormonal function of animals or human beings [12, 13, 14, 15]. Therefore, developing novel methods for determination of NP and detection of its damage to DNA are highly demanded.

Various instrumental techniques such as electrophoresis [16, 17, 18], high-performance liquid chromatography (HPLC) [19, 20, 21], photoelectrochemical methods [22, 23, 24] and fluorescence methods [25, 26, 27] have been reported for detection of DNA damage. Despite their sensitivity, these methods have some disadvantages such as complexity, long assay time, high cost and labor-intensive. Therefore, developing novel analytical methods which are simple, fast, cheap and sensitive are needed. Among the existing methods, electroanalytical techniques because of having high sensitivity, simplicity, rapid response and low-cost are preferable for detection of DNA damage [28, 29, 30, 31, 32, 33].

In fabrication of electrochemical biosensors, the platform of the

* Corresponding author.
** Corresponding author.
E-mail addresses: mahmoudroushani@yahoo.com (M. Roshani), ali.jalalvand1984@gmail.com (A.R. Jalalvand).

https://doi.org/10.1016/j.heliyon.2019.e02755
Received 1 September 2019; Received in revised form 3 October 2019; Accepted 28 October 2019

biosensor is usually modified with different modifiers to obtain more selectivity and sensitivity. Nanomaterials are promising candidates for fabricating electrochemical biosensing platforms and among the existing nanomaterials, gold nanoparticles (Au NPs) exhibit tremendous potential to improve the sensitivity and performance of electrochemical biosensors because of their unique physicochemical properties, high electric conductivity, large surface to volume ratio, good biocompatibility and nontoxic nature [34, 35, 36]. Chitosan (Chit) is a polysaccharide biopolymer with many remarkable features such as excellent film forming ability, high mechanical strength, high biocompatibility and high permeability toward water. Chit has a high sorption capacity for various materials and molecules due to the existence of reactive amino and hydroxyl functional groups. For these reasons, Chit as an efficient film has been widely used for chemical modifications of the electrode surface to construct electrochemical biosensors [37, 38, 39]. As a kind of carbon-based material, multi-walled carbon nanotubes (MWCNTs) as ideal supporting materials has received an increasing research interest due to their unique chemical and physical properties such as good biocompatibility, large specific surface area, electrical conductivity and chemical stability. Various molecules such as DNA molecule can interact physically with the MWCNTs surface through π–π stacking. Therefore, MWCNTs have been frequently used to immobilize a variety of species in fabrication of electrochemical biosensors [40, 41, 42]. Methylene blue (MB) is a derivative of anthraquinone which can intercalate into the double helix structure of DNA and can be used as an electroactive probe in fabrication of electrochemical biosensors for detection of DNA damage induced by damaging agents. After intercalation of the MB into the double helix structure of the DNA at the biosensor surface, the MB can be replaced by the damaging agent which affects the electrochemical response of the biosensor and allow us to monitor the DNA damage induced by the damaging agent.

In this work, we have developed a sensitive electrochemical biosensor to monitor the DNA damage induced by NP and the next section was focused on developing a novel electroanalytical methodology for sensitive determination of NP based on the outputs of previous section. To achieve these goals, a glassy carbon electrode (GCE) was chosen as the platform of the biosensor and layer-by-layer modification was applied to it. The first layer of the modification process was included drop-casting of Chit and then, electrodeposition of Au NPs onto Chit/GCE surface was performed. The next attempt was focused on landing of DNA-MWCNTs onto the surface of Au NPs/Chit/GCE which was performed by drop-casting of DNA-MWCNTs onto the electrode surface. Afterwards, the modified electrode was immersed into a MB solution which caused intercalation of MB into the double helix structure of DNA. Finally, the MB-DNA-MWCNTs/Au NPs/Chit/GCE was immersed into a NP solution and the DNA damage induced by NP was monitored in the redox-active probe $[Fe(CN)_6]^{3-/4-}$ solution by electrochemical impedance spectroscopy (EIS) based on faradaic impedance changes. The schematic representation of the fabrication procedure is shown in Scheme 1.

2. Experimental

2.1. Chemicals, solutions, software and instruments

The DNA, NP, MB and all other reagents used in this study such as $K_3Fe(CN)_6$, $K_4Fe(CN)_6$, H_3PO_4, NaH_2PO_4, Na_2HPO_4, NaOH, KCl, NaCl, acetic acid, gold (III) tetrachloride ($HAuCl_4$), MWCNTs and Chit were purchased from Sigma. The MWCNTs were purchased from Ionic Liquid Technologies. All the reagents were of analytical grade and used as received without further purification. Doubly distilled water (DDW) was used to prepare all the solutions. A phosphate buffer solution (PBS) with a concentration of 0.05 M was prepared by dissolution of suitable amounts of solid powders of NaH_2PO_4 and Na_2HPO_4 in DDW and its pH was adjusted at 7.4 by H_3PO_4 and NaOH. A solution of MWCNTs was prepared by dissolution of 15 mg of solid powder of MWCNTs in 1 mL DMF and then, ultrasonicated for 45 min. A Chit solution was prepared by dissolution of 10 mg Chit in 1 mL acetic acid and then, ultrasonicated for 30 min. A redox probe solution, $[Fe(CN)_6]^{3-/4-}$, with a concentration of 0.005 M was prepared in the PBS (0.05 M, pH 7.4). A MB solution with a concentration of 0.01 M was prepared in the PBS (0.05 M, pH 7.4). A solution of $HAuCl_4$ with a concentration of 1 mM was prepared in 0.025 M KCl. A DNA solution (1.0 mg mL^{-1}) was prepared by dissolving a suitable amount of solid powder of DNA in 0.05 M NaCl solution. To prepare DNA-MWCNTs gel-like mixture, 500 μL DNA solution (1.0 mg mL^{-1}) was added to 500 μL MWCNTs solution (1.0 mg mL^{-1}) and well mixed by hand-shaking.

The 3D structure of nanotubes was designed by Nanotube Modeler software (Fig. 1A-C) and the PDB file of DNA (PDB ID: 1BNA) was downloaded from Protein Data Bank (Fig. 1D). Nanotubes were then docked to the DNA using Molegro Virtual Docker (MVD) software. EQUISPEC as well-known hard-modeling chemometric algorithm was used to determine the binding constant of the complex formed upon interaction of NP with DNA.

All the electrochemical data were recorded by a 302N high performance Autolab controlled by a Nova software (Version 2.1). Electrochemical measurements were performed in an electrochemical cell where a GCE, an Ag/AgCl (satd. 3.0 M KCl) and a platinum wire were acted as working, reference and auxiliary electrode, respectively. A JENWAY-3345 pH-meter equipped with a combined glass electrode was used to pH adjustments. Scanning electron microscopy (SEM) images were taken by using a MIRA3TESCAN-XMU. Energy dispersive X-ray spectroscopy (EDS) were performed for elemental analysis by an EDS-integrated Hitachi S-4800.

2.2. Fabrication of the biosensor

Prior to the fabrication of the biosensor, the GCE as the platform of the biosensor was well polished by alumina on a silky pad, ultrasonicated in ethanol, rinsed with DDW and dried. To start fabrication of the biosensor, 10 μL of Chit solution was dropped onto the surface of the

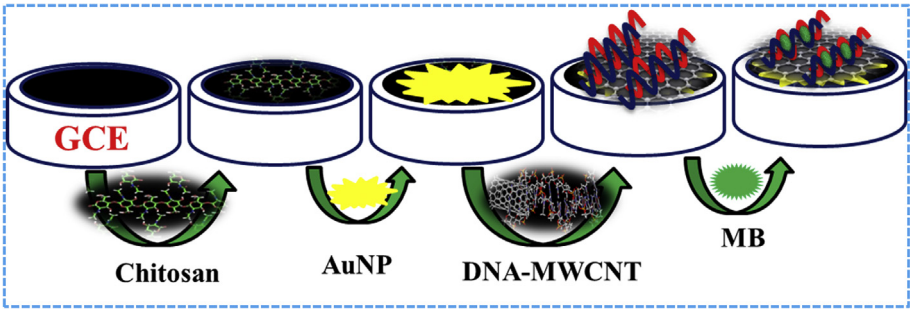

Scheme 1. The schematic representation of the fabrication of the proposed biosensor in this work.

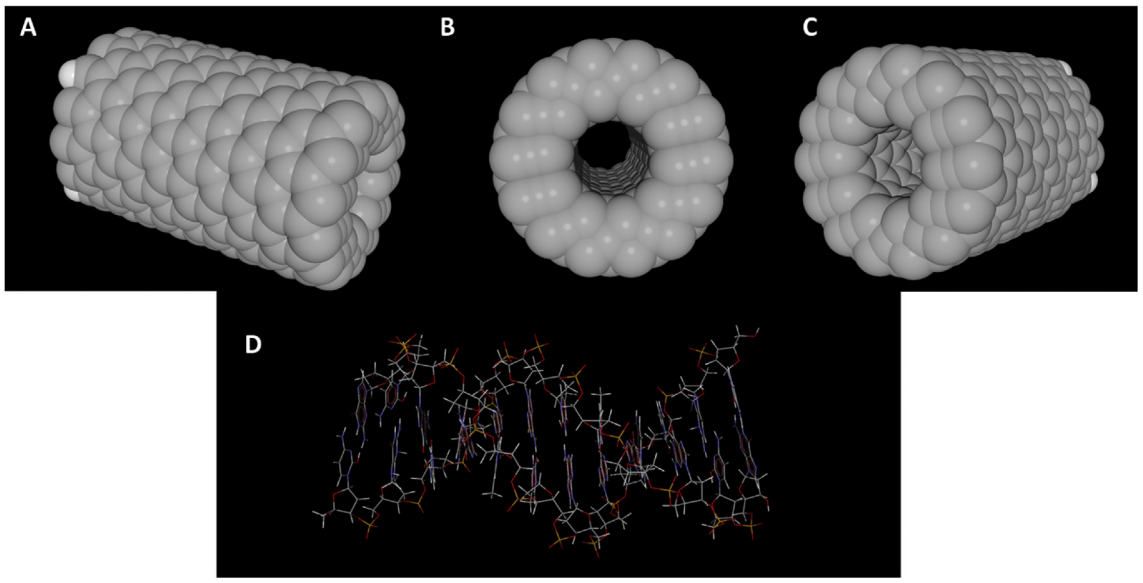

Fig. 1. (A)–(C) Different views of three-dimensional structure of the MWCNTs designed by Nanotube Modeler software represented by the CPK model and (D) molecular structure of DNA represented by the thin stick model.

cleaned GCE and kept at room temperature to be dried. The Chit/GCE was immersed into 1 mM $HAuCl_4$ solution and then, Au NPs were electrochemically deposited onto its surface by scanning potential from 0.0 to -1.5 V to fabricate Au NPs/Chit/GCE. Then, 10 μL DNA-MWCNTs was drop-casted onto the surface of the Au NPs/Chit/GCE and left to be dried at room temperature. Finally, for intercalation of the MB into the double helix structure of DNA molecules, the DNA-MWCNTs/Au NPs/Chit/GCE was immersed into 1 mM MB solution and then, the as-prepared MB/

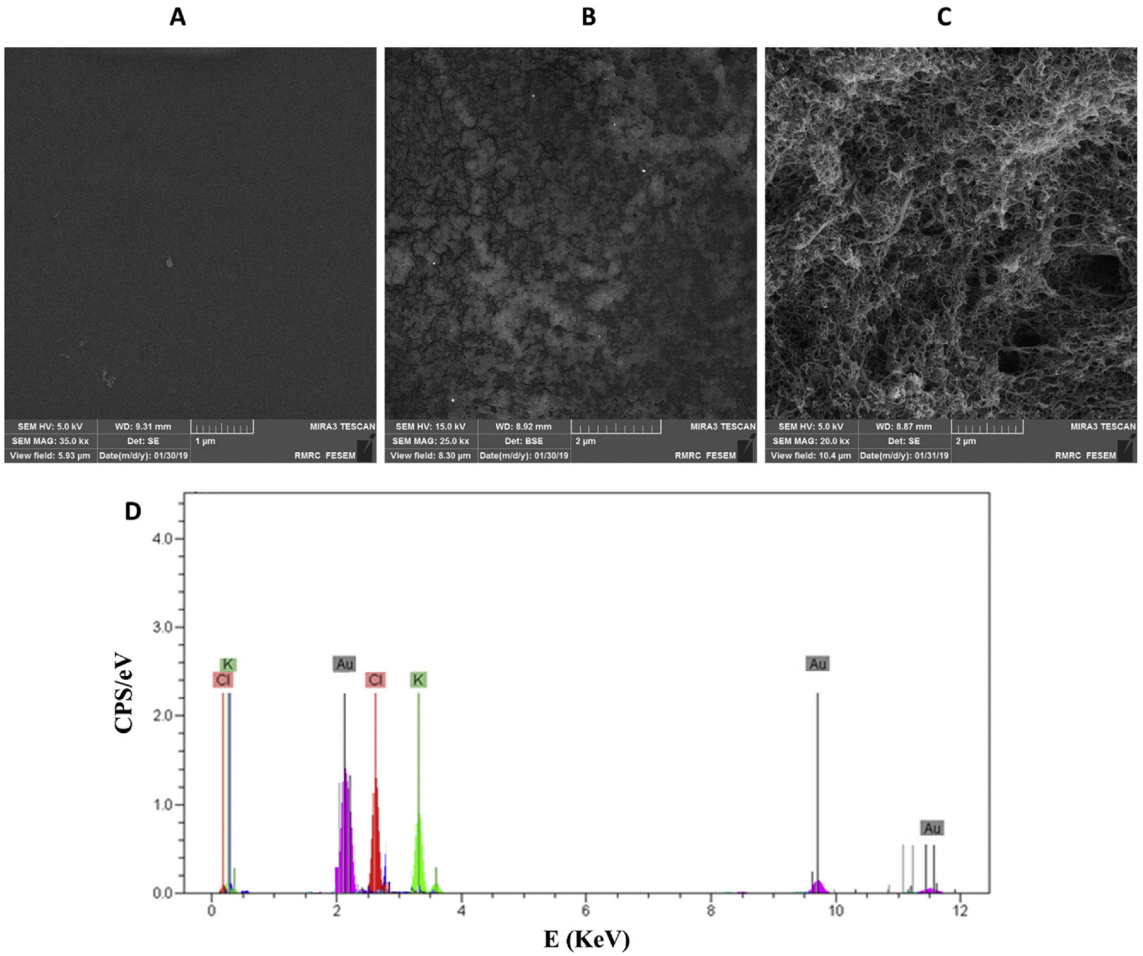

Fig. 2. SEM images of (A) Chit/GCE, (B) Au NPs/Chit/GCE and (C) DNA-MWCNTs/Au NPs/Chit/GCE. (D) Characterization peaks obtained by EDS.

DNA-MWCNTs/Au NPs/Chit/GCE was immersed into the PBS (0.05 M, pH = 7.4) solution containing 5 mM $K_3Fe(CN_6)/K_4Fe(CN_6)$ to record electrochemical responses.

3. Results and discussion

3.1. Characterization of the modifications

3.1.1. Morphological characterizations

The surface morphology of the GCE during stepwise modifications was characterized by SEM analysis, and results are illustrated in Fig. 2A-C. Fig. 2A shows the SEM image taken from the surface of Chit/GCE which confirms the existence of a layer on the surface of the electrode and further analysis of the electrode surface after electrodeposition of Au NPs showed a well distribution of Au NPs onto the electrode surface as could be seen in Fig. 2B. The next modification used to fabricate the biosensor was characterized by SEM analysis and the results are shown in Fig. 2C. As can be seen, the DNA-MWCNTs has formed a layer with a well distribution onto the surface of the electrode and the tubes of the MWCNTs have been twined around each other to form an interesting and pretty layer onto the electrode surface. Elemental analysis of Au NPs was carried out by EDS and the signature peaks which are shown in Fig. 2D which confirmed the successful electrodeposition of Au NPs onto the electrode surface.

3.1.2. Electrochemical characterizations

Electrochemical techniques are very useful to characterize the modifications applied to an electrode. Among the existing electrochemical techniques, CV and EIS are usually used to characterize the modifications [43]. Therefore, EIS and CV were used to characterize different modified electrodes in contact with 5 mM $[Fe(CN)_6]^{3-/4-}$ as probe redox. The CV responses related to different modified electrodes are shown in Fig. 3A. As can be seen, the GCE showed a well-defined CV (curve *a*) which its peak intensities were increased after its modification with Chit (curve *b*) which may be related to more positive charge at the surface of Chit and attracting the redox probe carrying negative charges. After

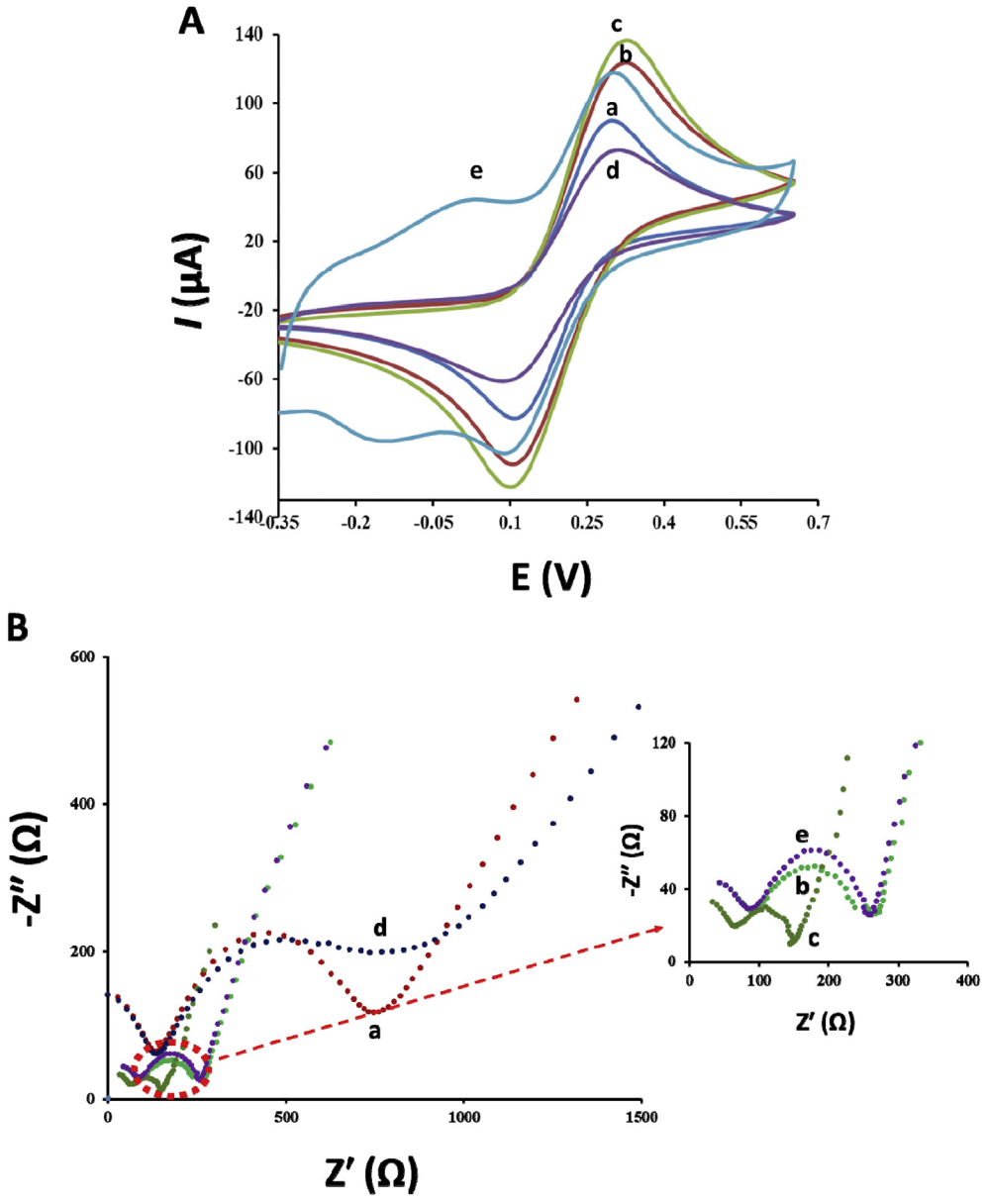

Fig. 3. (A) CVs and (B) EISs of (a) GCE, (b) Chit/GCE, (c) Au NPs/Chit/GCE, (d) DNA-MWCNTs/Au NPs/Chit/GCE, and (e) MB/DNA-MWCNTs/Au NPs/Chit/GCE. Enlargement of EIS of (c), (b) and (e) is shown as inset of (B). All the CVs and EISs were recorded in 5 mM $[Fe(CN)_6]^{3-/4-}$ as redox probe solution.

electrodeposition of Au NPs onto the surface of Chit/GCE, more enhancement of CV response was observed (curve *c*) which may be related to the more conductivity caused by the presence of Au NPs which provide a lot of new conduction pathways to facilitate electron transfer between electrode surface and electrolyte solution [44]. Drop-casting of DNA-MWCNTs onto the surface of Au NPs/Chit/GCE caused a weaker response (curve *d*) which may be related to the repulsion of the redox probe carrying negative charge by the negatively charged phosphate back-bone of the DNA immobilized on the surface of DNA-MWCNTs/Au NPs/Chit/GCE. Subsequently, by the incubation of DNA-MWCNTs/Au NPs/Chit/GCE into a MB solution and intercalation of MB molecules into the double helix structure of DNA biomacromolecules, the peak currents were increased (curve *e*) because, MB molecules have the positive charge and interaction of them with DNA caused their intercalation into the double helix structure of DNA molecules on the surface of electrode therefore, attraction of the redox probe molecules towards the electrode surface is occurred [45].

Modifications were further characterized by EIS and the results are shown in Fig. 3B. As can be seen, the diameter (charge transfer resistance, R_{ct}) of the EIS curve of the GCE (curve *a*) was decreased (curve *b*) by the presence of Chit onto its surface which was compatible with CV results. After electrodeposition of Au NPs, a further decrease in the R_{ct} was observed (curve *c*) which was related to the more electrical conductivity of the Au NPs/Chit/GCE than Chit/GCE. By the presence of DNA-MWCNTs at the surface of Au NPs/Chit/GCE, a significant increase in R_{ct} was observed (curve *d*) which may be related to the fact that the negatively charged phosphate backbone of the DNA molecules caused an electrostatic repulsion to $[Fe(CN)_6]^{3-/4-}$ which decreased the access of the redox probe molecules to the electrode surface. Finally, by the incubation of the DNA-MWCNTs/Au NPs/Chit/GCE with a MB solution, the R_{ct} was decreased (curve *e*) which may be related to the presence of MB molecules with positive charge which caused an electrostatic attraction between the electrode surface and redox probe molecules.

3.2. Computational supporting evidence

In this section, docking studies helped us to have insights into the interactions between DNA and MWCNTs which can support the experimental results. Here, the MVD software was used to realize the binding mode of MWCNTs at the DNA. Fig. 4 shows the groove binding of MWCNTs to the major groove of DNA. These results confirmed formation of DNA-MWCNTs nanobiocomposite from computational point of view which supports the possibility of using the DNA-MWCNTs nanobiocomposite for analytical purposes.

In order to compute the binding constant related to the complex formed upon interaction of NP with DNA, the DPV data related to the addition of NP in the range of 0–5×10^{-4} M to 5×10^{-4} M DNA were recorded (not shown) and by modeling the data by EQUISPEC as a well-known hard-modeling chemometric algorithm, the binding constant was calculated to be 3.11×10^{6} M^{-1}.

3.3. Influence of the different modified electrodes on the MB loading

In order to compare loading of MB onto different electrodes including DNA/GCE, DNA/Chit/GCE, DNA/Au NPs/Chit/GCE and DNA-MWCNTs/Au NPs/Chit/GCE, the EIS responses of different electrodes in 5 mM $[Fe(CN)_6]^{3-/4-}$ were recorded and the results are shown in Fig. 5A. As can be seen, the responses were apparently different and the EIS curve of the MB/DNA-MWCNTs/Au NPs/Chit/GCE (curve *d*) had the lowest R_{ct} among the tested electrodes which confirmed that it had the relatively highest MB loading. The results showed that the DNA-MWCNTs formed a nanobiocomposite which was a stable and suitable platform for loading of MB and facilitated interaction of MB with DNA. Therefore, choosing it for sensing the DNA damage induced by NP due to showing sharp changes in its response in the presence of NP was preferred.

3.4. Influence of time of incubation with MB and NP

In order to find excellent efficiency of the designed biosensing system, the time of incubation of DNA-MWCNTs/Au NPs/Chit/GCE with MB and NP solutions as important parameters affecting the biosensor response, were investigated by the EIS method. To achieve this goal, the DNA-MWCNTs/Au NPs/Chit/GCE was prepared and immersed into a 1 mM MB solution with different incubation times ranging in 30–180 min and the EIS responses were recorded. Our records confirmed that the ΔR_{ct} ($\Delta R_{ct} = R_{ct}(t)\text{-}R_{ct}(0)$, where $R_{ct}(0)$ and $R_{ct}(t)$ are the diameter of the EIS curves of the DNA-MWCNTs/Au NPs/Chit/GCE without incubation with MB and incubation with 1 mM MB at different incubation times (*t*), respectively) was increased with the increase of the time of incubation with MB from 30 min to 120 min, and then was unchanged for the prolonging time (not shown). Therefore, 120 min was selected as the optimal incubation time with MB and used for our next studies. As mentioned above, the time of incubation of biosensor with NP is an important factor which can affect the biosensor response therefore, it was investigated by immersing of MB/DNA-MWCNTs/Au NPs/Chit/GCE into a 1 mM NP solution for different incubation times ranging in 10–100 min. Then, the EIS response of the MB/DNA-MWCNTs/Au NPs/Chit/GCE in the redox probe at the different incubation times were recorded and ΔR_{ct} ($\Delta R_{ct} = R_{ct}(t)\text{-}R_{ct}(0)$, where $R_{ct}(0)$ and $R_{ct}(t)$ are the diameter of the EIS curves of the DNA-MWCNTs/Au NPs/Chit/GCE without MB and treating with 1 mM NP at different incubation times (*t*), respectively) was increased with increasing time of incubation with NP from 10 min to 60 min, and then equilibrated to the constant value (not shown). Therefore, 60 min was chosen as the optimal time for incubation of the biosensor with NP.

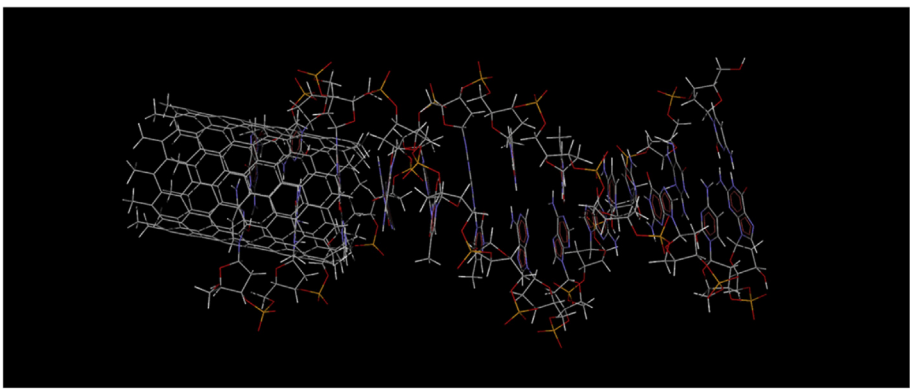

Fig. 4. Results of molecular modeling related to the groove binding of MWCNTs to the major groove of DNA.

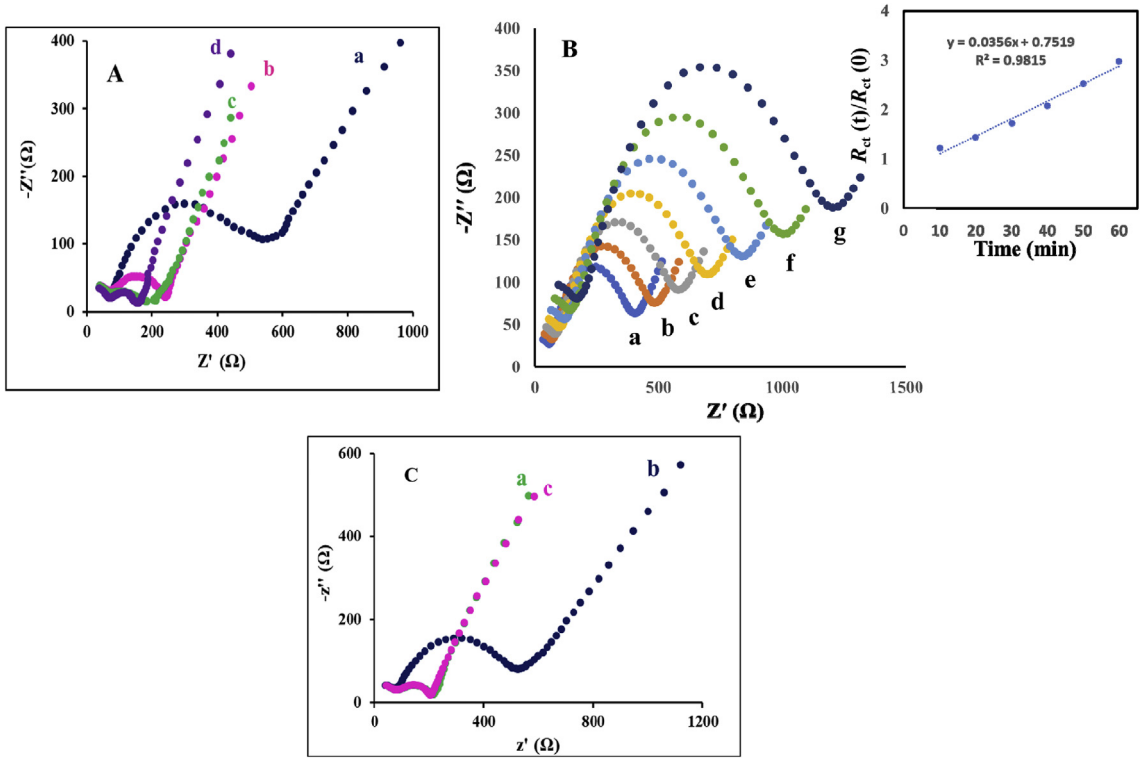

Fig. 5. (A) The EIS curves of different electrodes in 5 mM $[Fe(CN)_6]^{3-/4-}$: (a) MB/DNA/GCE, (b) MB/DNA/Chit/GCE, (c) MB/DNA/Au NPs/Chit/GCE, and (d) MB/DNA-MWCNTs/Au NPs/Chit/GCE. (B) The EIS responses of MB/DNA-MWCNTs/Au NPs/Chit/GCE without treating with NP (curve *a*) and upon different treating times with 0.5 mM NP ranging in 10–60 (curves b-g). (C) Investigation of the generation/regeneration of the MB/DNA-MWCNTs/Au NPs/Chit/GCE: recorded EIS curves of DNA-MWCNTs/Au NPs/Chit/GCE in 5 mM $[Fe(CN)_6]^{3-/4-}$ after (a) loading, (b) releasing and (c) reloading of the MB.

In order to investigate the extent of the DNA damage induced by NP, the damage rate of the DNA was estimated by the EIS. To achieve this goal, the EIS responses of MB/DNA-MWCNTs/Au NPs/Chit/GCE upon different treating times with 0.5 mM NP ranging in 10–60 min with an increment of 10 min were recorded which are shown in Fig. 5B. The ratio of $R_{ct}(t)/R_{ct}(0)$ ($R_{ct}(0)$ corresponds to the EIS curve of the biosensor without treating with NP and $R_{ct}(t)$ corresponds to the EIS curves of the biosensor after 10, 20, 30, 40, 50 and 60 min incubation with NP (curves *b-g*)) was plotted versus time of incubation with 0.5 mM NP which is shown as the inset of Fig. 5B. As can be seen, a linear behavior was observed. Slope of the plot gave the rate of damage which was 0.0356 min^{-1}.

3.5. Testing generation/regeneration of the MB/DNA-MWCNTs/Au NPs/Chit/GCE

In order to examine the generation/regeneration of the MB/DNA-MWCNTs/Au NPs/Chit/GCE, it was immersed into a 1 mM MB solution for 120 min and then, its EIS response was recorded by immersing it into a 5 mM $[Fe(CN)_6]^{3-/4-}$ (loading MB, Fig. 5C, curve *a*). Then, the MB/DNA-MWCNTs/Au NPs/Chit/GCE was immersed into the PBS (0.05 M, pH 7.4) for 120 min to release MB and its EIS response was recorded in 5.0 mM $[Fe(CN)_6]^{3-/4-}$ (releasing MB, Fig. 5C, curve *b*). As can be seen, the R_{ct} was increased which was related to the releasing some MB molecules. By releasing some MB molecules from the biosensor surface, some positive charges are missed which causes the existence of more negative charges at the biosensor surface therefore, repulsion of the redox probe molecules can be occurred and increasing the R_{ct} could be seen. The next attempt was focused on re-immersing the electrode into a 1 mM MB solution for 120 min and recording its EIS response in the redox probe solution (reloading MB, Fig. 5C, curve *c*). As can be seen, the R_{ct} was decreased due to the increasing the positive charge at the electrode surface which caused electrostatic attraction of redox probe molecules carrying negative charges. The results mentioned above confirmed that the biosensor response had a good generation/regeneration ability.

3.6. Impedimetric detection of the DNA damage

To verify the performance of the MB/DNA-MWCNTs/Au NPs/Chit/GCE as the fabricated biosensor for detecting DNA damage induced by NP, its EIS responses after incubation with different concentrations of NP ranging in 0.01–128.61 μM were recorded under the optimal experimental conditions. To achieve this goal, the biosensor was incubated with different concentrations of NP for 60 min and then, its EIS responses were recorded which are shown in Fig. 6A. As can be seen, by immersing the MB/DNA-MWCNTs/Au NPs/Chit/GCE into solutions of NP with different concentrations, the R_{ct} was increased which was occurred because of the insertion of NPs into the DNA and reducing its charge transport. Insertion of the NPs into DNA structure may cause a more negative charge on the DNA surface which hinders accessibility of the $[Fe(CN)_6]^{3-/4-}$ anion to the biosensor surface. In order to develop a novel electroanalytical methodology for determination of NP according to the EIS data recorded for detection of DNA damage induced by NP, ΔR_{ct} values ($\Delta R_{ct} = R_{ct} - Rct^0$, where R_{ct}^0 and R_{ct} are the diameter of the EIS curve of the biosensor in the absence and presence of NP, respectively) were regressed on NP concentrations to build a calibration curve which can be seen in Fig. 6B. The results showed that the EIS responses of the biosensor were linearly changed over two concentration ranges of NP including 0.01 μM–3.61 μM and 3.61 μM–128.61 μM. The calibration curve obeyed from equations ΔR_{ct} (Ω) = 14.501x + 12.136 (R^2 = 0.9804) and ΔR_{ct} (Ω) = 0.8491x + 63.803 (R^2 = 0.9951) and limit of detection (LOD) was calculated according to IUPAC recommendations ($3S_b/b$, where S_b is the standard deviation (n = 6) of the blanks, and *b* is the slope value of the calibration graph) which was 3.5 nM.

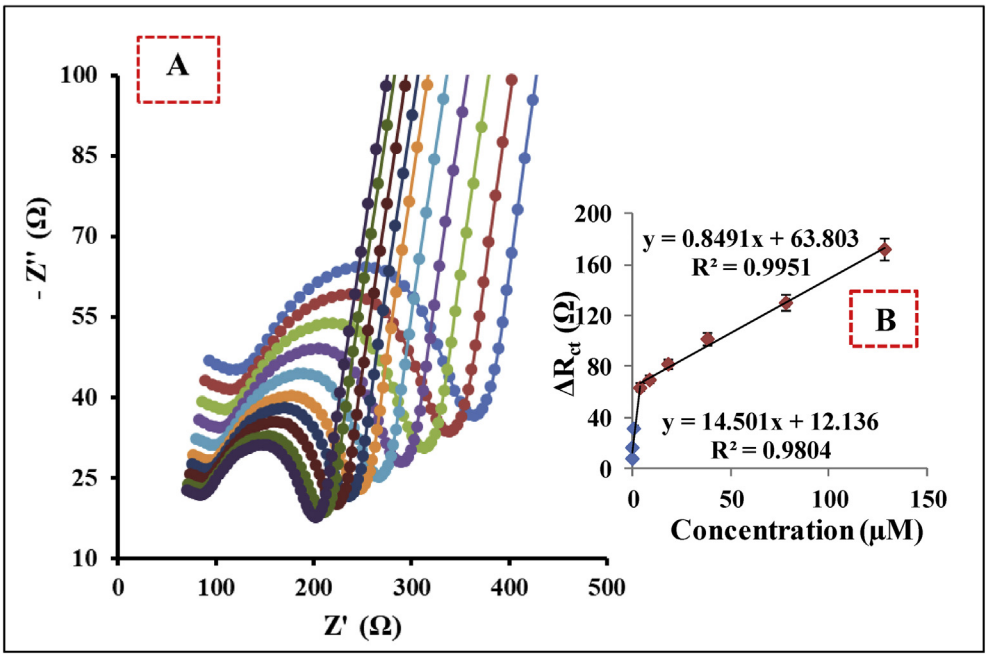

Fig. 6. The EIS curves of the MB/DNA-MWCNTs/Au NPs/Chit/GCE in 5 mM $[Fe(CN)_6]^{3-/4-}$ after incubation with different concentrations of NP ranging in 0.01–128.61 μM for 60 min. Inset shows the calibration graph obtained from linear regression of ΔR_{ct} values on NP concentrations.

3.7. Stability, repeatability and reproducibility

To evaluate the stability of the fabricated biosensor, its EIS responses in 5 mM $[Fe(CN)_6]^{3-/4-}$ after immersing it into a 50 μM NP solution for 60 min were recorded and then, the biosensor was stored in the PBS (0.05 M, pH 7.4) at 4 °C for 30 days. After this time, the EIS response of the biosensor was recorded and the results exhibited that the biosensor was able to retain 97.8% of its initial response which confirmed that the biosensor response had a good stability. The repeatability of the developed biosensor was examined by applying it to the determination of 50 μM NP for six times during a day and the results showed a relative standard deviation (*RSD*) of 3.66% which confirmed that the biosensor response was repeatable. The reproducibility of the proposed biosensor was investigated by using five biosensors fabricated under the same conditions. These biosensors were applied to the detection of the DNA damage induced by 50 μM NP and a *RSD* of 4.13% was calculated which confirmed that the biosensor response was reproducible.

3.8. Comparison with the previous works published in the literature

In this section, we have collected the results of the previous works published in the literature to compare our work with them and the information has been collected in Table 1. As can be seen, the biosensor proposed in this study was more stable than the reported biosensors by the previous works which may be related to integration of experimental and computational evidence to design and fabricate the biosensor as found by the previous works [52, 53, 54, 55, 56, 57, 58, 59, 60, 61, 62, 63, 64].

Table 1
A comparison study between different electrochemical approaches for detection of DNA damage.

Sensor	Method	Damaging reagent	Long term stability	Ref.
CS/ds-DNA/Ag-PGL/GCE	LSV	Fe^{2+}/H_2O_2	15 days	[46]
DNA–XOD/GCE	SWV	Xanthine/$FeSO_4$	7 days	[47]
DNA–XOD/GCE	SWV	$FeSO_4$/glucose	-	[48]
dsDNA/GCE	SWV	Fe^{2+}/EDTA/H_2O_2	-	[6]
(MWCNTs/PDDA/ds-DNA)$_2$/PGE	DPV	Cr(VI)/GSH/H_2O_2	-	[49]
(PDDA/dsDNA)3/GCE	CV	V_2O_5nanobelts/HCl/H_2O_2	30 days	[50]
DNA/GCE	SWV	Fe^{2+}/H_2O_2	-	[51]
DNA/AuNPs/SPGE	EIS	$CuSO_4/H_2O_2$/AA	21 days	[7]
dsDNA/GO-CS/AuNPs/GCE	EIS and DPV	NP, BPA and OP	15 days	[45]
MB/DNA-MWCNTs/Au NPs/Chit/GCE	EIS	NP	30 Days	This work

PDDA: poly (diallyldimethylammoniumchloride); PGE: pencil graphite electrode; GSH: glutathione (γ-l-glutamyl-l-cysteinyl-glycine); MB: methylene blue; BPA: bisphenol A; OP: 4-t-octylphenol; GO: graphene oxide; CS: chitosan; PGL: poly l-glutamic acid; LSV: linear sweep voltammetry; SWV: square wave voltammetry; DPV: differential pulse voltammetry.

4. Conclusions

In this work, a novel biosensor was fabricated based on layer-by-layer modification of a GCE with MB/DNA-MWCNTs/Au NPs/Chit to detection of DNA damage induced by NP. After characterization of the modifications by CV, EIS, SEM and theoretical methods, the operating conditions were optimized and then, under optimal conditions the biosensor was incubated with NP and its EIS response was recorded. The results showed that the EIS response of the biosensor was increased in the presence of NP which was occurred because of the insertion of NPs into the DNA and reducing its charge transport. Insertion of the NPs into DNA structure may cause a more negative charge on the DNA surface which hinders accessibility of the $[Fe(CN)_6]^{3-/4-}$ anion to the biosensor surface. Therefore, the EIS response of the biosensor was a useful technique to monitor the DNA damage induced by NP. The next step of our study was focused on developing a novel and indirect electroanalytical method for determination of NP based on the biosensor response to the DNA damage induced by NP. To achieve this goal, the ΔR_{ct} values were regressed on NP concentrations to build a calibration curve. Moreover, our records confirmed that the biosensor exhibited satisfactory stability and reproducibility for detecting DNA damage induced by NP.

Declarations

Author contribution statement

Ali R. Jalalvand: Conceived and designed the experiments; Analyzed and interpreted the data; Wrote the paper.

Kazhal Ghanbari: Conceived and designed the experiments; Performed the experiments; Analyzed and interpreted the data.

Mahmoud Roshani, Hector C. Goicoechea: Analyzed and interpreted the data; Contributed reagents, materials, analysis tools or data.

Funding statement

This research did not receive any specific grant from funding agencies in the public, commercial, or not-for-profit sectors.

Competing interest statement

The authors declare no conflict of interest.

Additional information

No additional information is available for this paper.

References

[1] G. Elgar, T. Vavouri, Tuning in to the signals: noncoding sequence conservation in vertebrate genomes, Trends Genet. 24 (2008) 344–352.
[2] P. Yakovchuk, E. Protozanova, M.D. Frank-Kamenetskii, Base-stacking and base-pairing contributions into thermal stability of the DNA double helix, Nucleic Acids Res. 34 (2006) 564–574.
[3] J. Kobierski, E. Lipiec, DNA structure change induced by guanosine radicals–A theoretical and spectroscopic study of proton radiation damage, J. Mol. Struct. 1178 (2019) 162–168.
[4] M.M. Zangeneh, H. Norouzi, M. Mahmoudi, H.C. Goicoechea, A.R. Jalalvand, Fabrication of a novel impedimetric biosensor for label free detection of DNA damage induced by doxorubicin, Int. J. Biol. Macromol. 124 (2019) 963–971.
[5] E. Heydari-Bafrooei, M. Amini, S. Saeednia, Electrochemical detection of DNA damage induced by Bleomycin in the presence of metal ions, J. Electroanal. Chem. 803 (2017) 104–110.
[6] A. Hájková, J. Barek, V. Vyskočil, Electrochemical DNA biosensor for detection of DNA damage induced by hydroxyl radicals, Bioelectrochemistry. 116 (2017) 1–9.
[7] S.Z. Mousavisani, J.B. Raoof, R. Ojani, Z. Bagheryan, An impedimetric biosensor for DNA damage detection and study of the protective effect of deferoxamine against DNA damage, Bioelectrochemistry. 122 (2018) 142–148.
[8] M. Valko, D. Leibfritz, J. Moncol, M.T.D. Cronin, M. Mazur, J. Telser, Free radicals and antioxidants in normal physiological functions and human disease, Int. J. Biochem. Cell Biol. 39 (2007) 44–84.
[9] D.K. La, J.A. Swenberg, DNA adducts: biological markers of exposure and potential applications to risk assessment, Mutat. Res. Genet. Toxicol. 365 (1996) 129–146.
[10] R. De Bont, N. Van Larebeke, Endogenous DNA damage in humans: a review of quantitative data, Mutagenesis. 19 (2004) 169–185.
[11] F.P. Guengerich, Interactions of carcinogen-bound DNA with individual DNA polymerases, Chem. Rev. 106 (2006) 420–452.
[12] H.-J. Chen, Z.-H. Zhang, R. Cai, X. Chen, Y.-N. Liu, W. Rao, S.-Z. Yao, Molecularly imprinted electrochemical sensor based on amine group modified graphene covalently linked electrode for 4-nonylphenol detection, Talanta. 115 (2013) 222–227.
[13] Q. Zhou, M. Lei, J. Li, K. Zhao, Y. Liu, Sensitive determination of bisphenol A, 4-nonylphenol and 4-octylphenol by magnetic solid phase extraction with Fe@ MgAl-LDH magnetic nanoparticles from environmental water samples, Separ. Purif. Technol. 182 (2017) 78–86.
[14] L. Zheng, C. Zhang, J. Ma, S. Hong, Y. She, A.M.A. EI-Aty, Y. He, H. Yu, H. Liu, J. Wang, Fabrication of a highly sensitive electrochemical sensor based on electropolymerized molecularly imprinted polymer hybrid nanocomposites for the determination of 4-nonylphenol in packaged milk samples, Anal. Biochem. 559 (2018) 44–50.
[15] P. Duan, B. Liu, C.L.M. Morais, J. Zhao, X. Li, J. Tu, W. Yang, C. Chen, M. Long, X. Feng, 4-Nonylphenol effects on rat testis and sertoli cells determined by spectrochemical techniques coupled with chemometric analysis, Chemosphere. 218 (2019) 64–75.
[16] K. Jung, R. Reszka, Mitochondria as subcellular targets for clinically useful anthracyclines, Adv. Drug Deliv. Rev. 49 (2001) 87–105.
[17] D.H. Atha, N. Ammanamanchi, M. Obadina, V. Reipa, Quantitative measurement of electrochemically induced DNA damage using capillary electrophoresis, J. Electrochem. Soc. 160 (2013) G3139–G3143.
[18] D. Anderson, J. Laubenthal, Analysis of DNA damage via single-cell electrophoresis, in: DNA Electrophor, Springer, 2013, pp. 209–218.
[19] M.K. Shigenaga, B.N. Ames, Assays for 8-hydroxy-2′-deoxyguanosine: a biomarker of in vivo oxidative DNA damage, Free Radic. Biol. Med. 10 (1991) 211–216.
[20] S. Loft, K. Vistisen, M. Ewertz, A. Tjønneland, K. Overvad, H.E. Poulsen, Oxidative DNA damage estimated by 8-hydroxydeoxyguanosine excretion in humans: influence of smoking, gender and body mass index, Carcinogenesis. 13 (1992) 2241–2247.
[21] J.W. Park, B.N. Ames, 7-Methylguanine adducts in DNA are normally present at high levels and increase on aging: analysis by HPLC with electrochemical detection, Proc. Natl. Acad. Sci. 85 (1988) 7467–7470.
[22] L.H. Hurley, DNA and its associated processes as targets for cancer therapy, Nat. Rev. Cancer. 2 (2002) 188–200.
[23] M. Liang, S. Jia, S. Zhu, L.H. Guo, Photoelectrochemical sensor for the rapid detection of in situ DNA damage induced by enzyme-catalyzed fenton reaction, Environ. Sci. Technol. 42 (2008) 635–639.
[24] S. Jia, M. Liang, L.H. Guo, Photoelectrochemical detection of oxidative DNA damage induced by Fenton reaction with low concentration and DNA-associated Fe2+, J. Phys. Chem. B. 112 (2008) 4461–4464.
[25] G. Quievryn, E. Peterson, J. Messer, A. Zhitkovich, Genotoxicity and mutagenicity of chromium (VI)/ascorbate-generated DNA adducts in human and bacterial cells, Biochemistry. 42 (2003) 1062–1070.
[26] Y. Zhou, X. Feng, D.W. Koh, Enhanced DNA accessibility and increased DNA damage induced by the absence of poly(ADP-ribose) hydrolysis, Biochemistry. 49 (2010) 7360–7366.
[27] F. Pu, Z. Huang, J. Ren, X. Qu, DNA/Ligand/Ion-Based ensemble for fluorescence turn on detection of cysteine and histidine with tunable dynamic range, Anal. Chem. 82 (2010) 8211–8216.
[28] J. Yang, Z. Zhang, J.F. Rusling, Detection of chemically-induced damage in layered DNA films with Co(bpy)33+ by square-wave voltammetry, Electroanalysis. 14 (2002) 1494–1500.
[29] J.F. Rusling, Sensors for toxicity of chemicals and oxidative stress based on electrochemical catalytic DNA oxidation, Biosens. Bioelectron. 20 (2004) 1022–1028.
[30] T. Liao, Y. Wang, X. Zhou, Y. Zhang, X. Liu, J. Du, X. Li, X. Lu, Detection of DNA damage induced by styrene oxide in dsDNA layer-by-layer films using adriamycin as electroactive probe, Colloids Surfaces B Biointerfaces. 76 (2010) 334–339.
[31] R.N. Goyal, S. Bishnoi, Sensitive voltammetric sensor for the determination of oxidative DNA damage in calf thymus DNA, Biosens. Bioelectron. 26 (2010) 463–469.
[32] S.C.B. Oliveira, A.M. Oliveira-Brett, In situ DNA oxidative damage by electrochemically generated hydroxyl free radicals on a boron-doped diamond electrode, Langmuir. 28 (2012) 4896–4901.
[33] Y. Ni, P. Wang, H. Song, X. Lin, S. Kokot, Electrochemical detection of benzo(a) pyrene and related DNA damage using DNA/hemin/nafion–graphene biosensor, Anal. Chim. Acta. 821 (2014) 34–40.
[34] S. Guo, E. Wang, Synthesis and electrochemical applications of gold nanoparticles, Anal. Chim. Acta. 598 (2007) 181–192.
[35] K. Saha, S.S. Agasti, C. Kim, X. Li, V.M. Rotello, Gold nanoparticles in chemical and biological sensing, Chem. Rev. 112 (2012) 2739–2779.
[36] C. Xie, H. Li, S. Li, J. Wu, Z. Zhang, Surface molecular self-assembly for organophosphate pesticide imprinting in electropolymerized poly(p-aminothiophenol) membranes on a gold nanoparticle modified glassy carbon electrode, Anal. Chem. 82 (2010) 241–249.
[37] M. Zhang, A. Smith, W. Gorski, Carbon Nanotube−Chitosan system for electrochemical sensing based on dehydrogenase enzymes, Anal. Chem. 76 (2004) 5045–5050.
[38] A.R. Jalalvand, Fabrication of a novel and high-performance amperometric sensor for highly sensitive determination of ochratoxin A in juice samples, Talanta. 188 (2018) 225–231.
[39] J.-Y. Sun, K.-J. Huang, S.-F. Zhao, Y. Fan, Z.-W. Wu, Direct electrochemistry and electrocatalysis of hemoglobin on chitosan-room temperature ionic liquid-TiO2-graphene nanocomposite film modified electrode, Bioelectrochemistry. 82 (2011) 125–130.
[40] S. Khezrian, A. Salimi, H. Teymourian, R. Hallaj, Label-free electrochemical IgE aptasensor based on covalent attachment of aptamer onto multiwalled carbon nanotubes/ionic liquid/chitosan nanocomposite modified electrode, Biosens. Bioelectron. 43 (2013) 218–225.
[41] G. Mohammadi, E. Faramarzi, M. Mahmoudi, S. Ghobadi, A.R. Ghiasvand, H.C. Goicoechea, A.R. Jalalvand, Chemometrics-assisted investigation of interactions of Tasmar with human serum albumin at a glassy carbon disk: application to electrochemical biosensing of electro-inactive serum albumin, J. Pharm. Biomed. Anal. 156 (2018) 23–35.
[42] K. Ghanbari, M. Roushani, A nanohybrid probe based on double recognition of an aptamer MIP grafted onto a MWCNTs-Chit nanocomposite for sensing hepatitis C virus core antigen, Sens. Actuators B Chem. 258 (2018) 1066–1071.
[43] J. Yang, S. Deng, J. Lei, H. Ju, S. Gunasekaran, Electrochemical synthesis of reduced graphene sheet–AuPd alloy nanoparticle composites for enzymatic biosensing, Biosens. Bioelectron. 29 (2011) 159–166.
[44] A.R. Jalalvand, H.C. Goicoechea, H.W. Gu, An interesting strategy devoted to fabrication of a novel and high performance amperometric sodium dithionite sensor, Microchem. J. 144 (2019) 6–12.
[45] X. Lin, Y. Ni, S. Kokot, An electrochemical DNA-sensor developed with the use of methylene blue as a redox indicator for the detection of DNA damage induced by endocrine-disrupting compounds, Anal. Chim. Acta. 867 (2015) 29–37.
[46] X. Wang, C. Jiao, Z. Yu, Electrochemical biosensor for assessment of the total antioxidant capacity of orange juice beverage based on the immobilizing DNA on a

poly lglutamic acid doped silver hybridized membrane, Sens. Actuators B Chem. 192 (2014) 628–633.
[47] H. Xiong, Y. Chen, X. Zhang, H. Gu, S. Wang, An electrochemical biosensor for the rapid detection of DNA damage induced by xanthine oxidase-catalyzed Fenton reaction, Sens. Actuators B Chem. 181 (2013) 85–91.
[48] Y. Chen, H. Xiong, X. Zhang, S. Wang, Electrochemical detection of in situ DNA damage induced by enzyme-catalyzed Fenton reaction. Part I: in phosphate buffer solution, Microchim. Acta. 178 (2012) 37–43.
[49] A.A. Ensafi, M. Amini, B. Rezaei, Detection of DNA damage induced by chromium/glutathione/H_2O_2 system at MWCNTs–poly (diallyldimethylammonium chloride) modified pencil graphite electrode using methylene blue as an electroactive probe, Sens. Actuators B Chem. 177 (2013) 862–870.
[50] W. Zhang, T. Yang, W. Li, G. Li, K. Jiao, Rapid and sensitive electrochemical sensing of DNA damage induced by V2O5 nanobelts/HCl/H_2O_2 system in natural dsDNA layerby-layer films, Biosens. Bioelectron. 25 (2010) 2370–2374.
[51] Y. Wang, H. Xiong, X. Zhang, S. Wang, Electrochemical biosensors for the detection of oxidative DNA damage induced by Fenton reagents in ionic liquid, Sens. Actuators B Chem. 161 (2012) 274–278.
[52] M.B. Gholivand, A.R. Jalalvand, H.C. Goicoechea, M. Omidi, Investigation of interaction of nuclear fast red with human serum albumin by experimental and computational approaches, Spectrochim. Acta. 115 (2013) 516–527.
[53] A.R. Jalalvand, S. Ghobadi, H.C. Goicoechea, H.W. Gu, E. Sanchooli, Investigation of interactions of Comtan with human serum albumin by mathematically modeled voltammetric data: a study from bio-interaction to biosensing, Bioelectrochemistry. 123 (2018) 162–172.
[54] M.B. Gholivand, A.R. Jalalvand, H.C. Goicoechea, Multivariate analysis for resolving interactions of carbidopa with dsDNA at a fullerene-C_{60}/GCE, Int. J. Biol. Macromol. 69 (2014) 369–381.
[55] M.B. Gholivand, A.R. Jalalvand, H.C. Goicoechea, R. Gargallo, T. Skov, Chemometrics: an important tool for monitoring interactions of vitamin B7 with bovine serum albumin with the aim of developing an efficient biosensing system for the analysis of protein, Talanta. 132 (2015) 354–365.
[56] M.B. Gholivand, A.R. Jalalvand, G. Paimard, H.C. Goicoechea, T. Skov, R. Farhadi, S. Ghobadi, N. Moradi, V. Nasirian, Fabrication of a novel naltrexone biosensor based on a computationally engineered nanobiocomposite, Int. J. Biol. Macromol. 70 (2014) 596–605.
[57] A.R. Jalalvand, A. Haseli, F. Farzadfar, H.C. Goicoechea, Fabrication of a novel biosensor for biosensing of bisphenol A and detection of its damage to DNA, Talanta. 201 (2019) 350–357.
[58] M.B. Gholivand, A.R. Jalalvand, H.C. Goicoechea, G. Paimard, T. Skov, Surface exploration of a room-temperature ionic liquid-chitin composite film decorated with electrochemically deposited PdFeNi trimetallic alloy nanoparticles by pattern recognition: an elegant approach to developing a novel biotin biosensor, Talanta. 131 (2015) 249–258.
[59] M.B. Gholivand, A.R. Jalalvand, H.C. Goicoechea, Developing a novel computationally designed impedimetric pregabalin biosensor, Electrochim. Acta. 133 (2014) 123–131.
[60] M.B. Gholivand, A.R. Jalalvand, H.C. Goicoechea, Computer-assisted electrochemical fabrication of a highly selective and sensitive amperometric nitrite sensor based on surface decoration of electrochemically reduced graphene oxide nanosheets with CoNi bimetallic alloy nanoparticles, Mater. Sci. Eng. C. 40 (2014) 109–120.
[61] M.B. Gholivand, A.R. Jalalvand, H.C. Goicoechea, T. Skov, Fabrication of an ultrasensitive impedimetric buprenorphine hydrochloride biosensor from computational and experimental angles, Talanta. 124 (2014) 27–35.
[62] A.R. Jalalvand, Fabrication of a novel and ultrasensitive label-free electrochemical aptasensor for detection of biomarker prostate specific antigen, Int. J. Biol. Macromol. 126 (2019) 1065–1073.
[63] R. Khodarahmi, S. Khateri, H. Adibi, V. Nasirian, M. Hedayati, E. Faramarzi, S. Soleimani, H.C. Goicoechea, A.R. Jalalvand, Chemometrical-electrochemical investigation for comparing inhibitory effects of quercetin and its sulfonamide derivative on human carbonic anhydrase II: theoretical and experimental evidence, Int. J. Biol. Macromol. 136 (2019) 377–385.
[64] A.R. Jalalvand, M.B. Gholivand, H.C. Goicoechea, T. Skov, K. Mansouri, Mimicking enzymatic effects of cytochrome P450 by an efficient biosensor for in vitro detection of DNA damage, Int. J. Biol. Macromol. 79 (2015) 1004–1010.